

Effectiveness of hematite derived from iron sand for adsorbing chromium (VI) – Characterization, isotherm models, and thermodynamics

Evi Susanti^{1*} , Assyadatina Fathimah², Fifia Zulti¹,
Eva Nafisyah¹, Rosidah¹, Sutanto Latief³

¹ Research Centre for Limnology and Water Resources, National Research and Innovation Agency, Republic of Indonesia, Jl. Raya Jakarta – Bogor KM. 46 Cibinong, Indonesia

² Student in the Department of Chemistry, Faculty of Mathematics and Sciences, Pakuan University, Bogor, Indonesia

³ Department of Chemistry, Faculty of Mathematics and Sciences, Pakuan University, Bogor, Indonesia

* Corresponding author's e-mail: evis001@brin.go.id

ABSTRACT

The industry has suffered major chromium wastewater issues. Chromium is a heavy metal that can threaten both nature and people's health. Adsorption is a simple, environmentally friendly, and effective process for removing chromium from wastewater. Iron sand is an alternate adsorbent that can adsorb chromium. The iron sand in this research originated from Sukabumi, Indonesia, with a hematite content of 63.335%. The goal of this study is to evaluate the adsorption mechanism of hematite based on adsorbent weight, Cr(VI) initial concentration, pH of the solution, and contact time. This study was conducted experimentally throughout multiple phases. First, hematite was characterized using XRD, BET, FTIR and XRF to assess crystal structure, mineral composition, surface area, functional groups and the percentage of hematite in iron sand. Subsequently, the pH and contact time were optimized. The highest adsorption capacity is then determined using the Langmuir and Freundlich isotherms. The study found that hematite has a surface area before and after adsorption of 619.486 m²/g and 334.783 m²/g, with XRD peaks at $2\theta = 33.037^\circ$ and 35.357° , Fe-O bonds with a wavelength of 647.17 cm⁻¹ and hematite content of 63.335%. Optimal Cr(VI) adsorption occurs at pH 1, with a contact time of 120 minutes, Cr(VI) concentration of 50 mg/L, 5.0 g mass of hematite, with an adsorption capacity (Q_e), and adsorption efficiency (%) of 3.83 mg/g and 75.95%. The Freundlich isotherm model accurately represents adsorption, revealing a heterogeneous surface. The linear equation of the Freundlich curve is $\text{Log } Q_e = 0.1152 \text{ Log } C_e + 0.6376$, $R^2 = 0.9999$, with the value of adsorption capacity (k_f) = 4.3411 mg/g and adsorption intensity (n) = 8.681. The enthalpy of adsorption (ΔH_{ads}) at a concentration of 20 mg/L, 2.5 g, pH 3, and 30 minutes is -95.852 kJ/mol, indicating chemisorption.

Keywords: Cr(VI), hematite, adsorption, optimization, isotherm, enthalpy.

INTRODUCTION

Industrial activities face serious waste problems related to chromium, due to its carcinogenic nature to humans based on Group I classification by the International Agency for Research on Cancer (IARC), and Group A inhalation carcinogen by the US Environmental Protection Agency (EPA). Hydrogen potential (pH) and oxidation numbers strongly influence the toxicity of Cr(VI) to aquatic organisms. Almost all Cr(VI) substances

are anions, readily adsorb in water, and are quite resilient, despite their strong oxidized properties in acidic conditions. The EPA establishes a maximum safe limit for Cr(VI) levels in water at 0.05 mg/L, while in wastewater is 0.1 mg/L for the electronics and galvanized electroplating industries. Increasing the number of contaminants in wastewater, such as Cr(VI), in high levels and accumulating them over time becomes cancerous, producing environmental concerns and sickness (Zeng and Duan, 2022; Farhan *et al.*, 2023).

The act of adsorption entails the formation of adsorbate substances within the sorbent. Since most adsorbents rely on active functional groups, the chemistry of the adsorbent affects the heavy metal adsorption method (Chakraborty *et al.*, 2020; Ugwu *et al.*, 2020). Indonesia possesses high-quality mineral iron resources, containing 17% primary iron ore, 8% iron sand, and 75% laterite iron ore (Sukirman *et al.*, 2018). Iron sand is found in the lowest sedimentary rocks and consists of a complex mixed with iron, cement, ink, and magnetic components (Fahlepy *et al.*, 2018; Togibasa, 2019). Iron sand generates complex compounds using a coordination covalent bond mechanism and is commonly employed as a complexing agent.

Chromium contamination in wastewater remains a critical environmental challenge, particularly due to its carcinogenic properties. Treatment technologies such as chemical precipitation, adsorption, solvent extraction, coagulation, flocculation, flotation, ion exchange, membrane filtration, and electrochemical reduction have been widely used to mitigate heavy metals contamination, including chromium (Peng and Guo, 2020; Gahrouei *et al.*, 2024). Iron oxide and manganese dioxide are among the most common adsorbents for heavy metal removal, but there has been limited exploration of naturally sourced iron sand as a high-potential adsorbent for Cr(VI) removal. Naturally occurring iron sand, contains hematite (Fe_2O_3), magnetite (Fe_3O_4), and other valuable elements like iron, zinc, nickel, and titanium (Rianna *et al.*, 2018), offers a sustainable and cost-effective alternative for Cr(VI) adsorption. The hematite-rich composition of iron sand makes it particularly effective in reducing Cr(VI) levels, adding novelty to this study approach. The study methodically investigates the effects of changing pH, adsorbent weight, initial Cr(VI) concentration, and contact time to maximize adsorption performance. Although it has been demonstrated that iron oxide's high surface-to-volume ratio improves its ability to adsorb metals such as chromium (Rettob, 2019; Sousa, 2021), this study is the first to characterize and assess natural iron sand for the removal of Cr(VI). The adsorption of Cr(VI) on iron oxide follows an isotherm model, where the temperature significantly affects the adsorption rates constant (k_1) and maximum capacity for adsorption (Q_c). To establish the most effective adsorption mechanism, the adsorption process using iron sand should be evaluated by

considering the adsorbent weight, initial Cr(VI) concentration, pH, and contact time.

MATERIALS AND METHODS

Characterization of iron sand

The samples that were prepared correctly were evaluated utilizing a Brunauer-Emmet-Teller (BET) Surface Area Analyzer (Quantachrome NovaWin2) and a gas sorption analyzer to determine specific surface area and porosity. Fourier transform infrared spectroscopy (FTIR) is used to identify groups of functional found on the surface of iron sand. Analysis of X-ray diffraction (XRD) to evaluate the crystalline configuration and mineral content using a diffractometer with X-rays and Cu-K α irradiation at a 2θ -angle range from 5 – 80° with a scan speed of $0.02^\circ/\text{second}$. X-ray fluorescence (XRF) analysis to quantify the percentage of Fe concentration in iron sand.

Batch adsorption experiments

Diphenyl carbazide solution is prepared by diluting 0.125 mg of diphenyl carbazide crystalline in 25 mL of acetone. A concentration of 500 mg/L Cr(VI) solutions was set up by digesting 1.414 g of $\text{K}_2\text{Cr}_2\text{O}_7$ crystals in water from distillations in a 1 L volumetric flask. A curve of the standard was obtained at a concentration Cr(VI) of 20, 35, 50, and 65 mg/L, and the intensity of absorbance was detected by applying a UV-Vis spectrophotometer 1800 Shimadzu at 540 nm.

The adsorption of Cr(VI) upon iron sand was studied utilizing the batch experimental approach. The impact of pH (1, 3, 5), adsorbent weight (2.5 and 5.0 grams), Cr(VI) concentrations (20, 35, 50, and 65 mg/L), and temperature (30° , 40° , 50° , and 60°C) were studied.

The research stages are as follows:

- To examine the impact of adsorbent weight, 2.5 and 5.0 grams of iron sands were tested with 50 mg/L Cr(VI) solutions at 30°C in Erlenmeyer. The Erlenmeyer was agitated red at 120 rotations per minute (rpm) during 24 hours of contact time. The procedure stated that the compositions were passed through filters and the Cr(VI) level in the filtrates was determined.
- To investigate the impact of pH, 2.5 grams of iron sand were immersed in 50 mg/L of

chromium solutions at varying pH levels 1, 3, and 5, then agitated on an orbital shaker at 120 rpm for 24 hours. The pH level of the solution was modified with 1 N HCl solution. The mixes were passed through filters and tested for remaining chromium levels. The effect of contact time was examined for the identical combinations at durations ranging from 0 to 24 hours.

- To investigate the impact of initial concentration, 2.5 grams of iron sand were mixed with 20.0 - 65.0 mg/L of Cr(VI) medium at pH 3.0 derived from $K_2Cr_2O_7$ in Erlenmeyer. The Erlenmeyer was rotated at 120 rpm for a 2-hour contact time. The reacted solution underwent filtering, and the Cr(VI) levels in the filtrate were determined. The quantity of adsorbed Cr(VI) was estimated by subtracting the initial concentration (C_i) and final levels (C_e).
- To investigate enthalpy adsorption, 2.5 grams of iron sand were mixed with 50 mg/L of Cr(VI) solution. Each Erlenmeyer was conditioned at temperatures of 30°, 40°, 50°, and 60 °C and stirred for 120 minutes.

Data analysis

Adsorption capacity (Q) and adsorption isotherm constant (k) were calculated utilizing the Langmuir and Freundlich isotherm model. Determination of adsorption capacity by applying this formula:

$$Q_e = V \frac{(C_i - C_e)}{m} \quad (1)$$

The percentage of sorption (%R) can be measured using this formula:

$$\%R = \frac{C_i - C_e}{C_i} \times 100\% \quad (2)$$

where: Q_e – adsorption capacity per adsorbent weight (mg/g); V – medium volume (L); C_i – ion concentration initially in the solution (mg/L); C_e – the equilibrium level of ions (mg/L); and m – quantity of the utilized mass in the sorption procedure (g)

The adsorption of solutes by the surface of a solid is applied by the Freundlich isotherm which is obtained experimentally in the following way of the equation (Cooney, 1999):

$$Q_e = k_f C_e^{1/n} \quad (3)$$

Logarithmic, the formula would be:

$$\text{Log } Q_e = \text{Log } k_f + \frac{1}{n} \text{Log } C_e \quad (4)$$

Table 1. Result of physical characterization of hematite by BET surface area

Parameter	Unit	Before adsorption	After adsorption
Surface area	m ² /g	619.486	334.783
Pore volume	cm ³ /g	6.591	3.404

The Langmuir isotherm is derived according to the equation (Langmuir, 1917):

$$Q = \frac{k_1 k_2 C}{1 + k_2 C} \quad (5)$$

The Langmuir equation can be reduced to the equation:

$$\frac{C_e}{Q_e} = \frac{1}{k_1 k_2} + \frac{1}{k_1} C \quad (6)$$

where: Q_e – amount of adsorbate adsorbed every milligram of adsorbent (mg/g); C_e – equilibrium levels of adsorbate in medium following sorption (mg/L); k , n , k_1 , k_2 – constant.

The adsorption enthalpy is determined by the linear equation between the plot of $\ln C_e$ against $1/T$.

$$\ln C_e = \frac{-\Delta H_{ads}}{R} \times \frac{1}{T} + \text{Constant} \quad (7)$$

$$b = \frac{\Delta H_{ads}}{R} \quad (8)$$

where: slope, a = intercept, and ΔH_{ads} = slope \times R.

RESULTS AND DISCUSSION

Characterization of hematite

Brunauer-Emmet-Teller (BET)

Hematite particles possessed an approximate size of 60 μ m and a surface area of 619.486 m²/g and 334.783 m²/g before and after adsorption (Table 1). The adsorbent’s surface area is proportional to its sorption ability (Weber, 1972). The surface area of hematite after adsorption is lower than before adsorption because the adsorbent surface has bonded with the adsorbate, thereby reducing the surface area of the adsorbent.

This is influenced by mesopores, which perform an essential part in adsorption because they create a vast surface area for interacting with adsorbate molecules. When the mesopores are filled with adsorbate, the effectiveness of the adsorbent’s surface area decreases, corresponding to the decrease in the surface area of iron sand

after adsorption. This occurs because the adsorbate molecules occupy the pores, reducing the area for further adsorption. According to research by Thommes *et al.* (2007), mesoporous characteristics such as pore size, distribution, and volume greatly influence mesoporous materials'

adsorption efficiency and capacity. The BET test results show that iron sand is a type III isotherm, meaning the adsorbent quantity increases as the pressure increases (Figure 1).

Fourier transform infrared spectroscopy (FTIR)

Figure 2 compares hematite before and after the adsorption process with a wavelength of 2519.04 cm^{-1} and 2518.03 cm^{-1} , which is the O-H stretching vibration of Fe-O. These results show that the hematite before adsorption is smaller than after adsorption (Karbeka *et al.*, 2020). A significant peak at 1693.65 cm^{-1} appears after adsorption, corresponding to the C=O stretching vibration, suggesting the involvement of carbonyl groups during the adsorption process. Additionally, the Fe-O bond, which is a key characteristic of hematite, shows stretching vibration at 652.32 cm^{-1} and shifts to 647.17 cm^{-1} after adsorption. Similar shifts are observed in the wavelengths 599.49 cm^{-1} and 596.97 cm^{-1} . The shifts indicated that Cr(VI) interacts with the Fe-O bonds, modifying the bonding environment on the hematite surface. The FTIR results clearly indicate that the

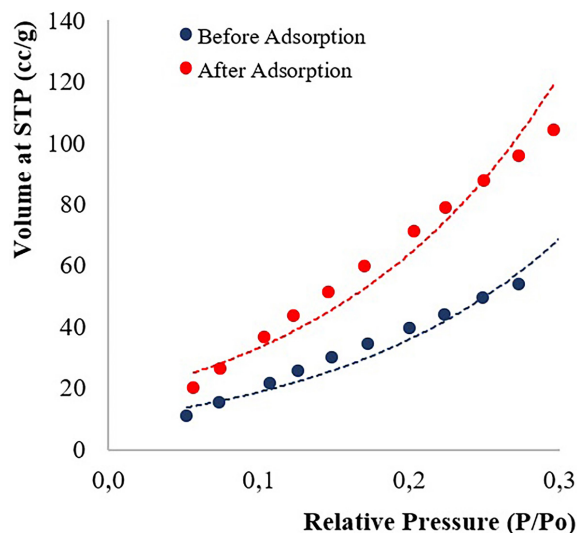


Figure 1. Isotherm plots pattern of hematite before and after adsorption

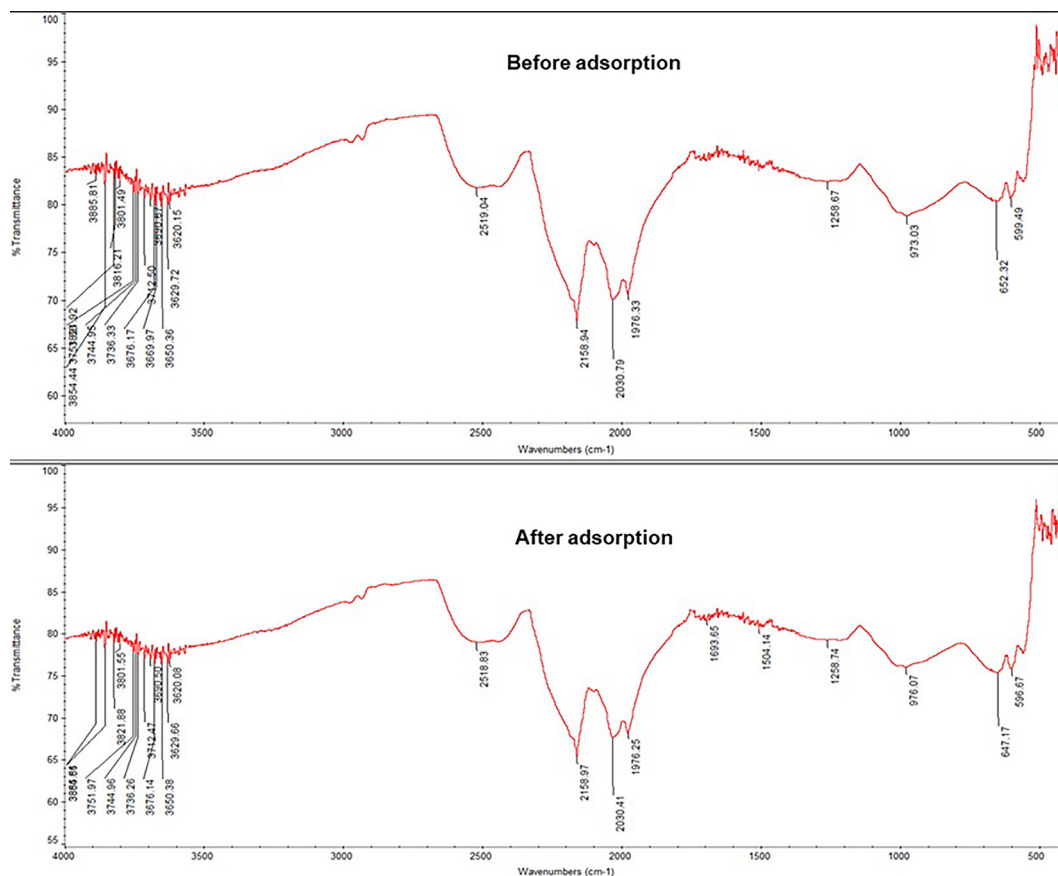


Figure 2. FTIR spectrum of hematite before and after adsorption

adsorption process was successful, as shown by the reduced transmittance after adsorption, which correlates with a greater presence of functional groups. This reduction in transmittance further confirms the involvement of O-H, Fe-O, and C=O functional groups in the adsorption process, reinforcing the effectiveness of hematite as an adsorbent for Cr(VI) removal.

X-ray diffraction (XRD)

The spectra show that the iron sand is crystalline, with a diffraction maximum, and has a sharp diffractogram peak (Figure 3). The peak of $2\theta = 18.290^\circ, 19.310^\circ, 27.893^\circ, 28.000^\circ, 30.053^\circ, 30.957^\circ, 32.718^\circ, 33.037^\circ, 35.357^\circ, 37.407^\circ, 42.543^\circ, 43.110^\circ, 53.331^\circ, 56.867^\circ, 62.670^\circ, \text{ and } 73.820^\circ$, with peaks intensity $2\theta = 27.893^\circ$ and 35.357° . The peaks of XRD characteristics at $2\theta = 30.08^\circ, 35.42^\circ, 43.11^\circ, 53.43^\circ, 56.75^\circ, \text{ and } 62.45^\circ$, indicate hematite (Fe_2O_3) referring to the peak characteristics of the Joint Committee on Powder Diffraction Standards (JCPDS) No 01-075-0449. Fe_2O_3 compound has a rhombohedral crystal structure with a crystallinity of 25.76% (Adegoke and Adekola, 2012; Selvasembian and Singh, 2022).

X-ray fluorescence (XRF)

The analysis of the XRF data corroborated the characterization of the sampel as a hematite. Concerning XRF measurements, the sample contained 63.335% Fe_2O_3 , Ti 7.019%, Co 1.200%, Mn 0.476%, V 0.443%, Ca 0.472%, Zn 0.060%, and several other minerals in small percentages.

Adsorption of Cr(VI) on hematite

Effect of weight, pH, and contact time

The experiment on the impact of adsorbent weight was carried out at pH 5, with a weight of 2.5 g, the capacity of adsorption (Q_e) attained 5.25 mg/g, and at a weight of 5.0 g, the capacity of adsorption (Q_e) was 2.26 mg/g (Figure 4). It is known that increasing the weight of the adsorbent utilized can increase the adsorption capacity and percentage of efficiency of Cr(VI). The adsorption percentage continued to rise at contact times of 5, 10, 15, 30, 45, 60 to 120 minutes. Extension up to 1440 minutes did not significantly increase adsorption efficiency.

The optimal contact time is reached as the adsorption mechanism approaches equilibrium and the adsorbate molecules penetrate the adsorbent pores. Increasing the contact time elevates the adsorption rate, however, the active adsorption decreases after passing equilibrium (Nafisyah *et al.*, 2023). This causes fewer metal ions to be absorbed and decreases response. The adsorption process reached equilibrium at 120 minutes, which indicated that the hematite had bound with the adsorbate and the increase in adsorption was no longer significant.

Determining the optimum weight is one of the important factors for defining the optimum weight is a crucial consideration when assessing the best circumstance in the mechanism for Cr (VI) adsorption utilizing iron sand as an adsorbent. Based on the data in Figure 8, it is known that increasing the weight of the adsorbent used can increase the

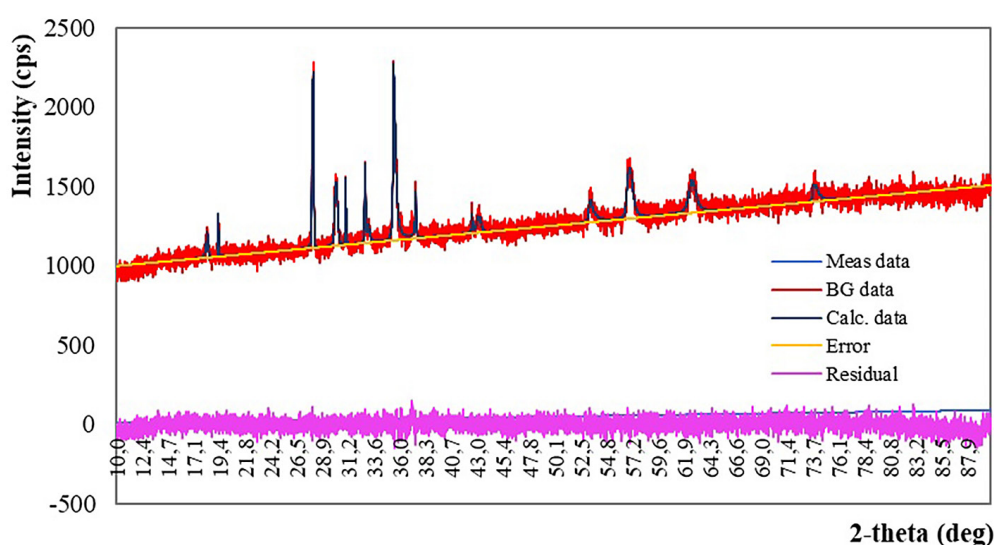


Figure 3. The diffractogram of hematite

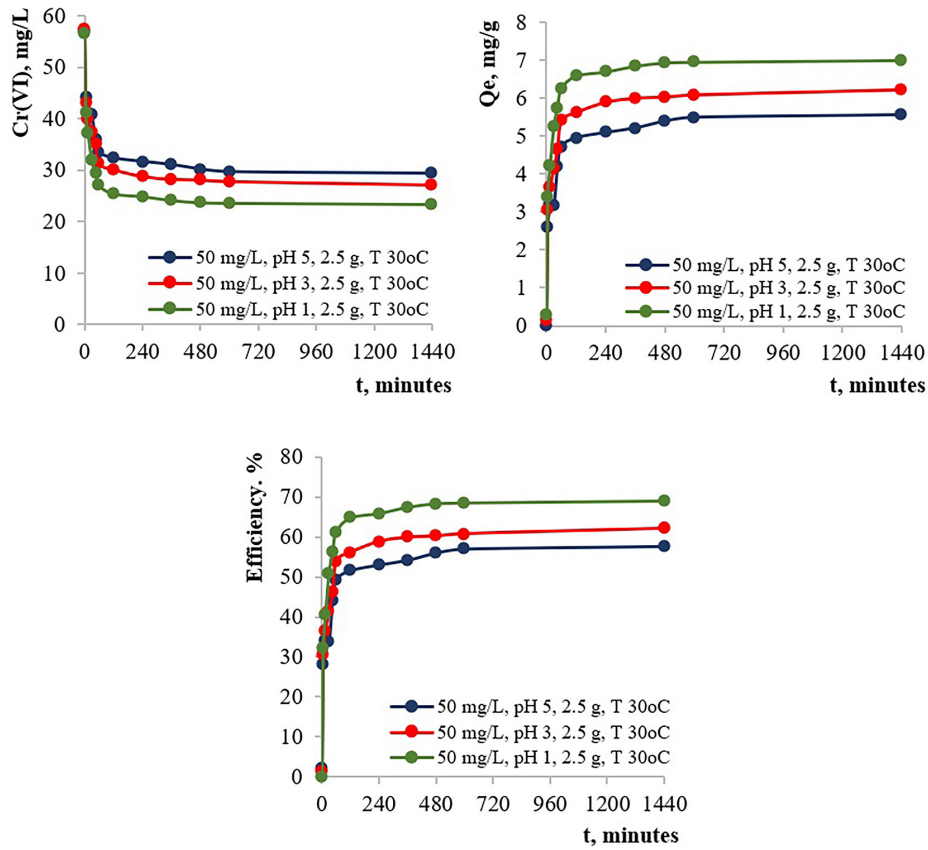


Figure 4. Effect of weight of 2.5 grams of hematite on the Cr(VI) adsorption in pH variation

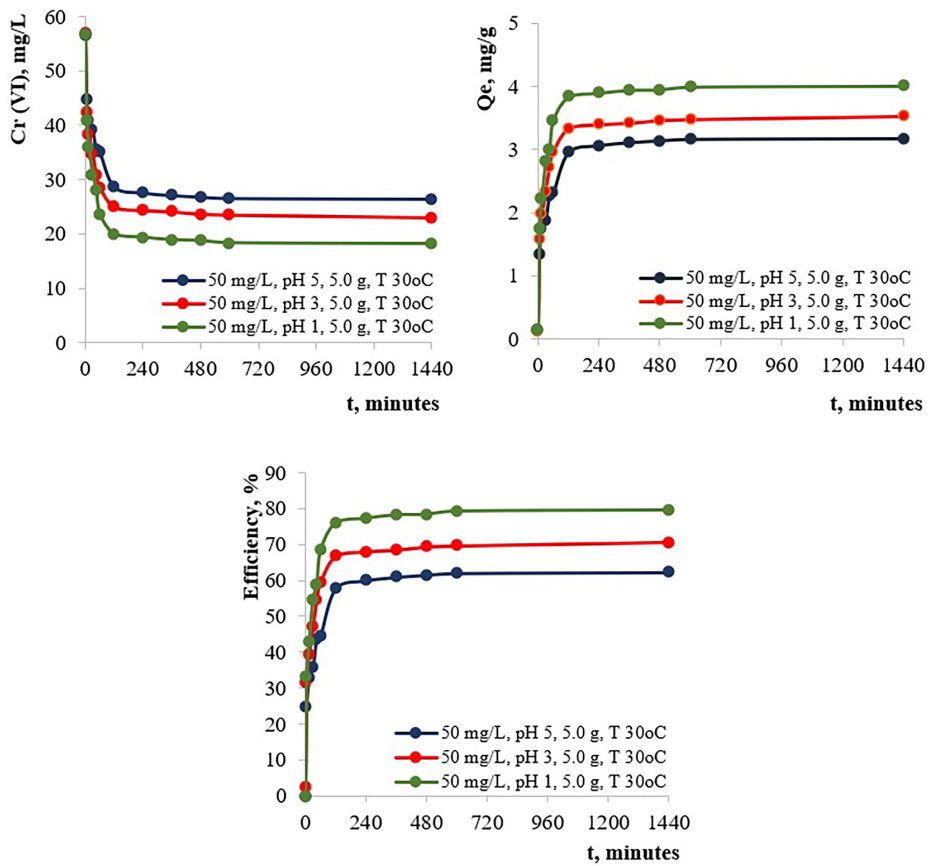


Figure 5. Effect of weight of 5.0 grams of hematite on the Cr(VI) adsorption in pH variation

capacity of adsorption, the addition of the weight of the adsorbent will also increase the adsorption capacity of the metals trapped.

The influence of pH variations on Cr(VI) adsorption is described in Figures 4 and Figure 5. The Cr(VI) adsorption capacity increases under acidic conditions (pH 1 and 3) compared to pH 5. At pH above 3, the amount of large ions OH⁻ rises, inhibiting the diffusion of chromate ions, resulting in a decrease in adsorption capacity. At pH 5, the availability of Cr (VI) ions is deficient so it is difficult to be absorbed by the adsorbent (Sulastri *et al.*, 2014).

The lowest adsorption of Cr(VI) ions occurs at pH 5 (Figure 6). At pH > 5, the availability of Cr (VI) ions will decrease. At this pH condition, there is competition between chromium species (HCrO₄⁻ and CrO₄²⁻) with OH⁻ ions, and the positive properties on the adsorbent surface decrease as protons decrease. At pH < 5, the dominating species is H₂Cr₂O₇. At alkaline pH, complexes of metal hydroxide may develop, reducing adsorption efficiency. The ideal pH during testing was

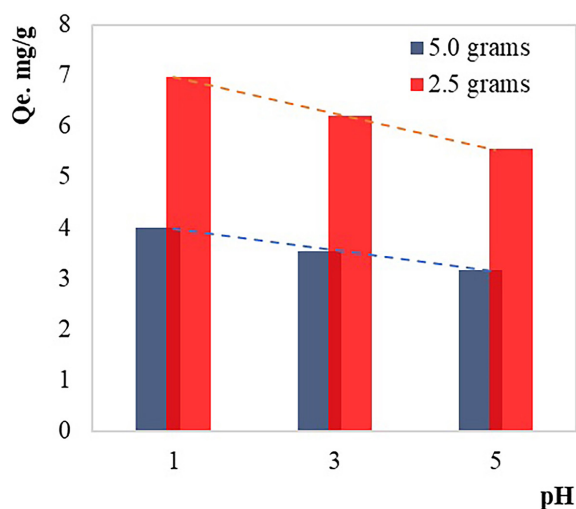


Figure 6. Effect of pH on the adsorption capacity of hematite

at pH 3 and pH 1. In acidic pH conditions, competitiveness among the analyte and hydrogen ions (H⁺) may interact with functional groups on the adsorbent's surface (Nafisyah *et al.*, 2023).

At pH 1 with a sample weight of 2.5 g, the adsorption capacity (Q_e) amounted to 6.23 mg/g, and at a weight of 5 g, the adsorption capacity (Q_e) was 3.83 mg/g. Meanwhile, at pH 3, weight of 2.5 g, the adsorption capacity (Q_e) is 5.62 mg/g, and at a weight of 5.0 g, the adsorption capacity (Q_e) is 3.33 mg/g. Optimal conditions are those at which an adsorbent can absorb the solution to the greatest extent possible. The capacity to adsorb a pollutant is influenced by pH, contact time, and weight adsorbent used. The higher the pH, the lower the absorption capacity at alkaline pH allowing the formation of metal hydroxide complexes which will degrade adsorption effectiveness. The best results are obtained when the study is performed at pH 3. In an acidic pH setting, ion competition allows the analyte and ion H⁺ to compete with functional groups on the outer layer of the adsorbent.

This research concluded that increasing the weight of the adsorbent used and the pH < 3 will increase the adsorption ability of the adsorbent. Optimum conditions were achieved with a weight of 5.0 g, pH 1, 120 minutes, at a level of 50 mg/L, with a capacity of adsorption (Q_e) and efficiency (%) of 3.83 mg/g and 75.95% (Table 2).

Adsorption isotherm

The isotherm assay was conducted utilizing hematite with a weight of 2.5 g, pH 3, and for 120 minutes, to determine how the initial concentrations influence the adsorption capacity (Q_e) and efficiency adsorption (%). The mechanism of hematite adsorption on Cr(IV) ions can be known from the adsorption isotherm type. Determination of the Cr(IV) adsorption isotherm was carried out by testing at several concentration levels to produce a

Table 2. The adsorption capacity and efficiency in each treatment

Time, minutes	pH	Q _e (mg/g)		Efficiency (%)	
		5.0 (g)	2.5 (g)	5.0 (g)	2.5 (g)
120 minutes	1	3.83	6.57	75.95	64.73
	3	3.33	5.62	66.67	56.18
	5	2.95	4.95	57.78	51.61
1444 minutes	1	4.01	6.98	79.57	68.95
	3	3.53	6.22	70.60	62.16
	5	3.17	5.55	62.31	57.64

linear curve of the Langmuir isotherm and Freundlich isotherm. Table 3 and Figure 7a show the Langmuir isotherm, and Table 4 and Figure 7b show the Freundlich isotherm curves obtained.

The linear equation obtained from the Langmuir isotherm curve by hematite, namely $C_e/Q_e = 1.6943 Q_e - 6.9079$, $R^2 = 0.8531$. Based on this equation, the value obtained is $q_m = 0.5902$ mg/g, and $k_L = 0.2453$ L/g. The linear equation of the Freundlich curve is $\text{Log } Q_e = 0.1152 \text{ Log } C_e + 0.6376$, $R^2 = 0.9999$, with the number of adsorption capacity (k_f) = 4.3411 mg/g and adsorption intensity (n) = 8.681. A greater value of k_f suggests a higher adsorption capacity (Selvasembian and Singh, 2022). The n value denotes the energetic heterogeneity of sites for adsorption and specifies the level of nonlinearity among levels of medium and adsorption. As n is greater than 1, then adsorption is a chemisorption (Brazesh *et al.*, 2021). The $R^2 = 0.9999$, shows that Cr(VI) adsorption using

hematite follows the Freundlich isotherm model, which describes adsorption on surfaces with heterogeneous properties and can work at various adsorbate concentrations. This model does not assume monolayer saturation, which is more realistic for many real systems, including adsorption on iron sand (Foo and Hameed, 2010).

The enthalpy of adsorption

The thermodynamic parameters are determined is the adsorption enthalpy (ΔH_{ads}). Adsorption enthalpy (ΔH_{ads}) and the $\ln C_e$ versus $1/T$ curve are illustrated within Table 4 and Figure 8. Adsorption enthalpy is determined by the degree of intensity of the molecular interactions among the adsorbent surface with the adsorbate. From the experimental results, it was obtained that $\Delta H_{\text{ads}} = 8.314 \text{ kJ/mol} \times 11529 = -95.852 \text{ kJ/mol}$, which demonstrates the adsorption of hematite on Cr(VI)

Table 3. The isotherm of Langmuir and Freundlich

Conc. Cr(VI) mg/L	Initial Conc. (C ₀) mg/L	Final Conc. (C _e) mg/L	ΔC	% ER	Q _e	Langmuir	Freundlich	
						C _e /Q _e	log Q _e	log C _e
20	19.764	0.375	19.389	98.10	3.878	0.0967	0.589	-0.426
35	34.631	7.315	27.316	78.88	5.463	1.3390	0.737	0.864
50	49.402	19.039	30.363	61.46	6.073	3.1352	0.783	1.280
65	64.203	31.778	32.425	50.50	6.485	4.9002	0.812	1.502

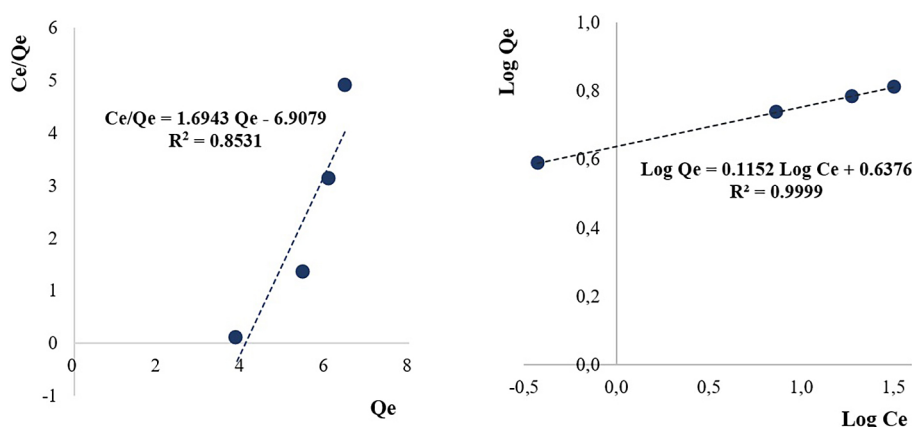


Figure 7. The linear graphic of Langmuir (a) and Freundlich isotherms (b)

Table 4. The enthalpy of adsorption (ΔH_{ads}) at a concentration of 20 mg/L, 2.5 g, pH 3, and 30 minutes

Temperature (K)	Initial Conc., C ₀ (mg/L)	Final Conc., C _e (mg/L)	x/m (mg/g)	$\ln C_e$	1/T
303	19.311	6.043	1.1166	1.7989	0.0033
313	18.976	3.195	1.3444	1.1616	0.0032
323	19.332	0.749	1.5401	-0.2890	0.0031
333	19.545	0.214	1.5829	-1.5418	0.0030

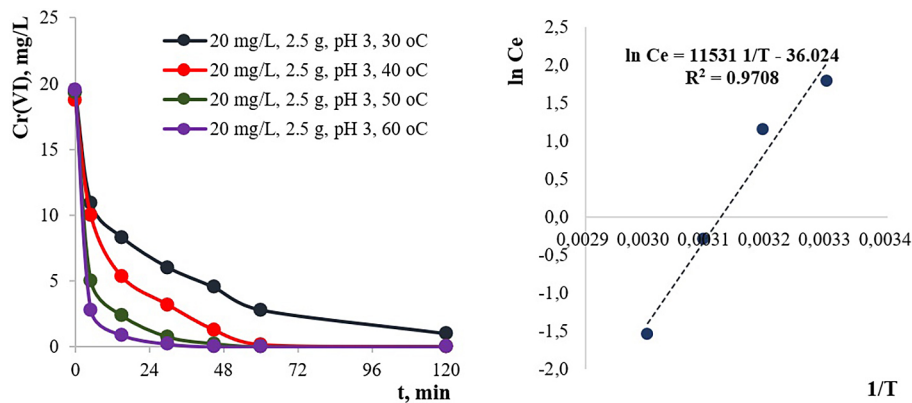


Figure 8. The enthalpy of adsorption and relationship curve between $\ln C_e$ and $1/T$, at a concentration of 20 mg/L in 30°, 40°, 50°, and 60 °C

is a type of chemisorption. Kralik (2014) classifies chemisorption in the range of 40–400 kJ/mol depending on the type of chemical bond formed, while physisorption with adsorption energy in the range of 10–40 kJ/mol due to Vander Walls force. Chemical adsorption is very possible due to Fe and Cr is both transition metals. Transition metals can form complex compounds by providing empty orbitals to accept electron pair donors, thus forming covalent bond coordination.

The ${}_{24}\text{Cr}$ atom has an electron configuration of $[\text{Ar}] 3d^5 4s^1$. In its Cr^{6+} form, the electron configuration becomes $[\text{Ar}] 3d^0 4s^0$, allowing it to accept six lone pairs of electrons to form a coordinating covalent bond. Similarly, the ${}_{26}\text{Fe}$ atom has an electronic configuration $[\text{Ar}] 3d^6 4s^2$. In its Fe^{3+} form, the electronic configuration changes to $[\text{Ar}] 3d^5 4s^0$, providing an empty $d^2 sp^3$ orbital, which enables it to accept six electron pairs for coordinating covalent bonding. The oxygen atoms in each of these structures have lone pairs of electrons that can be donated to metal atoms to organize coordinating covalent bonds.

Future research recommendations

Iron sand is abundant in countries rich in mineral resources and volcanic landscapes, offering promising potential as an adsorbent for treating wastewater containing Cr(VI). The widespread availability of iron sand provides an efficient and sustainable alternative to wastewater treatment, supporting green technology that aligns with Indonesia's local resources. Future research should focus on scaling up from batch to large-scale application, emphasizing efficiency, scalability, and operational ease. Developing a continuous flow

system with a stable flow rate can be explored using various reactor types, including packed bed reactors (PBR) (Obanijesu *et al.*, 2003), moving bed biofilm reactors (MBBR) (Tchobanoglous *et al.*, 2014), fluidized bed reactors (FBR) (Papirio, 2012) and hybrid reactors, combining adsorption with other treatments, such as photocatalysts or electrochemistry processes (Chen *et al.*, 2017), allow simultaneous oxidation and adsorption, enhancing the Cr(VI) reduction rate and overall efficiency.

For industrial, iron sand may offer a more affordable adsorbent than specialized materials. Reduced costs make this method attractive to industrial managing large-scale effluent volumes. This method scalability with continuous flow potential by adapting the process to continuous flow reactors, industries can treat Cr(VI) contaminated wastewater more efficiently on a large scale. The dual action of hematite in the iron sand facilitates Cr(VI) reduction and adsorption, which could enhance removal efficiency and decrease overall processing time, particularly beneficial for industries needing consistent Cr(VI) levels. These aspects highlight how the method's design aligns with industrial needs for economical, scalable, and sustainable Cr(VI) remediation solutions.

CONCLUSIONS

The characteristics of iron sand as an adsorbent were obtained from the BET test results. The difference in surface area of iron sand before adsorption was found to be 619.486 m^2/g to 334.783 m^2/g . In XRD testing, peaks were obtained at intensity $2\theta = 33.037^\circ$ and 35.357° . FTIR obtained

Fe-O bond stretching at wavelengths 647.17 cm^{-1} and 596.97 cm^{-1} which shows typical Fe_2O_3 , with a Fe content of 63.335%. The ability of hematite to adsorb Cr(VI) under optimal weight conditions adsorbent 5.0 g, pH 1 which occurs within 120 minutes with initial concentration of Cr(VI) 50 mg/L. The Q_m value was obtained at 3.83 mg/g and adsorption efficiency of 75.95%. Hematite shows effective adsorption ability for Cr(VI), with the Freundlich isotherm model as the best representation of the data adsorption, indicating surface heterogeneity. In determining enthalpy, at a level of 20 mg/L, 2.5 g, pH 3, and 30 minutes, the adsorption obtained was $\Delta H_{\text{ads}} = -95.852$ kJ/mol. These findings prove the adsorption of hematite on Cr(VI) is included in the type of chemisorption.

Acknowledgments

The Deputy for Earth Science, National Research and Innovation Agency, Republic of Indonesia, approved this project as part of the Water Resources and National Priority Lakes Management Program 2023. The authors also thank the Advanced Characterization Physics Laboratories Serpong and Bandung, as well as E-Layanan Sains, the National Research and Innovation Agency (BRIN), for their facilities, scientific and technical support.

REFERENCES

- Adegoke, H.I., Adekola, F.A. (2012). Equilibrium sorption of hexavalent chromium from aqueous solution using synthetic hematite. *Colloid J.* 74, 420–426. <https://doi.org/10.1134/S1061933X12040035>
- Brazesh B., Mousavi, S.M., Zarei, M., Ghaedi, M., Bahrani, S., Hashemi, S.A. (2021). Chapter 9 Biosorption. *Interface Science and Technology* 33, 587–628. <https://doi.org/10.1016/B978-0-12-818805-7.00003-5>
- Chakraborty, R., Asthana, A., Singh, A. K., Jain, B., & Susan, A. B. H. (2020). Adsorption of heavy metal ions by various low-cost adsorbents: a review. *International Journal of Environmental Analytical Chemistry*, 102(2), 342–379. <https://doi.org/10.1080/03067319.2020.1722811>
- Chen, J.P., Wang, L.K., Wang, M.S., Hung, Y., Shammas, N.K. (2017). Remediation of heavy metals in the environment. London: CRC Press.
- Cooney, D.O. (1999). Adsorption design for wastewater treatment. Lewis Publishers, CRC Press LLC.
- Fahlepy, M.R., Tiwow, V.A., Subaer. (2018). Characterization of magnetite (Fe_3O_4) minerals from natural iron sand of Bonto Kanang Village Takalar for ink powder (toner) application. *Journal of Physics: Conference Series* 997 012036 <https://doi.org/10.1088/1742-6596/997/1/012036>
- Farhan, A., Zulfiqar, M., Samiah, et al. (2023). Removal of toxic metals from water by nanocomposites through advanced remediation processes and photocatalytic oxidation. *Curr Pollution Rep* 9, 338–358. <https://doi.org/10.1007/s40726-023-00253-y>
- Foo, K.Y., Hameed, B.H. (2010). Insights into the modeling of adsorption isotherm systems. *Chemical Engineering J.* 156(1), 2–10. <https://doi.org/10.1016/j.cej.2009.09.013>
- Gahrouei A.E., Rezapour, A., Pirooz, M., Pourebrahimi, S. (2024). From classic to cutting-edge solutions: A comprehensive review of materials and methods for heavy metal removal from water environments. *Desalination & Water Treatment* 319(100446) <https://doi.org/10.1016/j.dwt.2024.100446>
- Karbeka, M., Koly, F.V.L., Tellu, N.M. (2020). Karakterisasi sifat kemagnetan pasir besi Pantai Puntaru Kabupetn Alor-NTT. *Lantanida Journal* 8(2), 96–188. [10.22373/lj.v8i2.7867](https://doi.org/10.22373/lj.v8i2.7867)
- Kralik, M. (2014). Adsorption, chemisorption, and catalyst. *Chemical Papers* 68(12) 10.2478/s11696-014-0624-9
- Langmuir, I. (1917). The constitution and fundamental properties of solids and liquids. II Liquids. *Journal of the American Chemical Society* 39(9), 1848–1906. <https://doi.org/10.1021/ja02254a006>
- Nafisyah, E., Arrisujaya, D., Susanti, E. (2023). The utilization of water hyacinth (*Eichhornia crassipes*) harvested from the phytoremediation process as activated carbon in Cr(VI) adsorption. *IOP Conference Series: Earth and Environmental Science* 1211(1). <https://doi.org/10.1088/1755-1315/1211/1/012019>
- Obanijesu, E.O., Bello, O., Osinowo, F.A.O., Macaulay, S.R.A. 2004. Development of a packed-bed reactor for the recovery of metals from industrial wastewater. *Int. J. Env. And Pollution* 22(6). <https://doi.org/10.1504/IJEP.2004.006048>
- Papirio, S. (2012). Fluidized-bed bioreactor applications for the treatment of metal-, sulfate- and nitrate-contaminated mine waters. Thesis. Università degli Studi di Cassino e del Lazio Meridionale. 190.
- Peng, H., Guo, J. (2020). Removal of chromium from wastewater by membrane filtration, chemical precipitation, ion exchange, adsorption electrocoagulation, electrochemical reduction, electrodialysis, electrodeionization, photocatalysis, and nanotechnology: a review. *Environ Chem Lett* 18, 2055–2068. <https://doi.org/10.1007/s10311-020-01058-x>
- Rettob, A. (2019). Characterization of iron sand

- magnetic materials coated with 2-amino benzimidazole modified silica via green process. *IOP Conf. Ser.: Earth Environ. Sci.* 235, 012075 <https://doi.org/10.1088/1755-1315/235/1/012075>
18. Rianna, M., Sembiring, T., Situmorang, M., Kurniawan, C., Setiadi, E. A., Tetuko, A. P., & Sebayang, P. (2018). Characterization of natural iron sand from Kata Beach, West Sumatra with high energy milling (Hem). *Jurnal Natural*, 18(2), 97–100. <https://doi.org/10.24815/jn.v18i2.11163>
 19. Selvasembian, R., Singh, P. (2022). Biosorption of wastewater contaminants. USA: John Wiley & Sons Ltd. 296.
 20. Sousa, D.B.S.A.B. (2021). Assessing the potential use of water treatment sludge containing activated carbon for the removal of emerging pollutants. Portugal: Universidade NOVA de Lisboa.
 21. Sulastri, S., Nuryono, Kartini, I., Kunarti, E.S. (2014). Kinetika dan Keseimbangan Adsorpsi Ion Kromium (III) dalam Larutan pada Senyawa Silika dan Modifikasi Silika Hasil Sintesis dari Abu Sekam Padi. Fakultas Matematika dan Ilmu Pengetahuan Alam, Universitas Negeri Yogyakarta.
 22. Sukirman, E., Sarwanto, Y., Insani, A., Rina, M., Purwanto, A. (2018). Magnetic structure of magnetite phase of iron sand retrieved from Banten, Indonesia. *Journal of Physics: Conference Series*, 1091(1). <https://doi.org/10.1088/17426596/1091/1/012007>
 23. Tchobanoglous, G., Stensel, H.D., Tsuchihashi, R., Abu-Orf, M., Bowden, G., Pfrang, W. (2014). Wastewater engineering treatment and resource recovery. *Fifth Edition. 1.* US: McGraw-Hill International Edition.
 24. Thommes, Matthias, Kaneko, Katsumi, Neimark, Alexander V., Olivier, James P., Rodriguez-Reinoso, Francisco, Rouquerol, Jean and Sing, Kenneth S.W. (2015). Physisorption of gases, with special reference to the evaluation of surface area and pore size distribution. *Pure and Applied Chemistry*, 87(9–10), 1051–1069. <https://doi.org/10.1515/pac-2014-1117>
 25. Togibasa, O., Akbar, M., Pratama, A., Bijaksana, S. (2019). Distribution of magnetic susceptibility of natural iron sand in the Sarmi Coast Area. *Journal of Physics: Conference Series 1204*, 012074 <https://doi.org/10.1088/1742-6596/1204/1/012074>
 26. Weber, Jr. W.J. (1977). Physics chemical process for water quality control. New York: John Wiley Interscience. <https://doi.org/10.1002/aic.690190245>
 27. Zheng, Z., & Duan, X. (2021). Mitigating the health effects of aqueous Cr(VI) with iron-modified biochar. *International Journal of Environmental Research and Public Health*, 19(3), 1481. <https://doi.org/10.3390/ijerph19031481>
 28. Ugwu, E.I, Tursunov, O., Kodirov, D., Shaker, L.M., Al-Amiery, A.A., Yangibaeva, I., Shavkarov, F. (2020). Adsorption mechanisms for heavy metal removal using low-cost adsorbents: A review. *IOP Conference Series: Earth and Environmental Science* 614, 012166. <https://doi.org/10.1088/1755-1315/614/1/012166>